

Anisotropic electron-phonon coupling on a two-dimensional circular Fermi contour

TeYu Chien,¹ Emile D. L. Rienks,² Maria Fuglsang Jensen,² Philip Hofmann,² and E. W. Plummer^{1,3}

¹*Department of Physics and Astronomy, The University of Tennessee, Knoxville, Tennessee 37996-1200, USA*

²*Institute for Storage Ring Facilities and Interdisciplinary Nanoscience Center (iNANO), University of Aarhus, 8000 Aarhus C, Denmark*

³*Department of Physics and Astronomy, Louisiana State University, Baton Rouge, Louisiana 70803, USA*

(Received 29 November 2009; published 31 December 2009)

Angle-resolved photoemission reveals that the electron-phonon coupling (EPC) around the circular Fermi contour of the Be(0001) $\bar{\Gamma}$ surface state is strongly anisotropic. The mass enhancement parameter λ is found to range from values of ~ 1 , along high-symmetry directions, to ~ 0.6 in between in stark contrast to the theoretical calculations. Given the simplicity of this system it furnishes an ideal prototype for unraveling the origin of anisotropic EPC in two-dimensional materials.

DOI: [10.1103/PhysRevB.80.241416](https://doi.org/10.1103/PhysRevB.80.241416)

PACS number(s): 71.38.Cn, 73.20.At, 79.60.Bm

One of the grand challenges in material science is to understand the remarkable properties emerging from complex correlations and to control these properties for technological applications. In the family of correlated electron materials (CEMs) the complexity is intimately related to the coexistence of competing nearly degenerate states, which couple simultaneously active degrees of freedom—charge, lattice, orbital, and spin. Electron-boson coupling (EBC), of which electron-phonon coupling (EPC) is a special case, is driving functionalities such as high- T_c superconductivity and “colossal” magnetoresistance.¹

The possibility of anisotropic EBC is crucially important for these phenomena. The quantity of interest is not the average EBC strength but its precise dependence on direction and the Fermi wave vector k_F . However, at this point little is known about the potentially anisotropic character of many-body interactions in complex materials. This is partly because of the fact that different interactions are simultaneously present, making it difficult to disentangle them, and partly because the Fermi surfaces are already anisotropic. The experiments cannot disentangle the effects from different bosonic modes so understanding of EBC has relied upon theory to determine the magnitude and directional dependence of EPC. Density-functional theory (DFT) is considered as the “standard model” to compute EPC and phonon dispersions. But a recent theoretical paper has questioned the validity of DFT when calculating EPC in two-dimensional (2D) systems: “failure of local-density approximation and generalized gradient approximation DFT functionals in graphene and graphite.”² A failure of DFT in reduced dimensional systems would have dramatic implications on our understanding of CEMs.

What is called for is a system with a much simpler electronic structure and only one type of bosonic excitation. Here, we report on such a system, the quasi-two-dimensional surface state on the Be(0001) where anisotropic EPC exists even for a circular Fermi contour. This system can serve as an ideal test case for theory. In contrast to what is reported for graphene and graphite,² *ab initio* DFT calculations for Be surfaces reproduce both the measured geometric and electronic structures³ as well as the surface phonon dispersion.⁴ At the present time, DFT calculations for the EPC on Be(0001) do not reproduce the measurements.⁵ There seems to be a problem theoretically when the surface states become

more localized at the surface, i.e., 2D in character.

Using beryllium surface states as a test system has a number of advantages. The first is the electronic simplicity of Be, which permits an accurate description of the electronic,⁶ structural, and dynamic^{4,7} properties by DFT. The second advantage is the strong EPC [range from 0.7 to 1.18 (Refs. 8–12)] and high phonon energies (up to ~ 85 meV),⁷ due to strong bonding in beryllium and the small atomic mass. Consequently, the effect of the EPC can be observed over a wide energy range, relaxing the requirements on the experimental energy resolution. Closely related to this is the high Debye temperature of beryllium, which means that the data can be interpreted as if they were taken at $T=0$ K to a good approximation, even if the actual experiment was not performed at a very low temperatures. Finally, the (0001) surface of beryllium supports a simple free-electron-like surface state which is centered on the zone center $\bar{\Gamma}$ and has a Fermi contour that is circular within $\sim 1\%$ (Ref. 13) with a Fermi wave vector length of $\sim 0.94 \text{ \AA}^{-1}$.

Given these favorable conditions, it is not surprising that the nature of EPC for this surface state has been investigated experimentally^{8–12} and theoretically.¹⁴ But the state of affairs with respect to the strength of the EPC is somewhat inconclusive. Early angle-resolved photoemission spectroscopy (ARPES) measurements near the Fermi level indicated anomalously large EPC.¹⁰ However, subsequent reports have significantly widened the range of experimental λ values (defined as $\lambda = m_{eff}/m_0 - 1$) by almost a factor of 2, spanning the range from 0.7 to 1.18.^{8–12} The original DFT calculation reported a value of λ in the middle of this range,¹⁴ but subsequent calculations by this group now show that $\lambda = 0.44$, which is out of the experimental reported range.⁵ In this Rapid Communication, we resolve this inconsistency in the published experimental results for the mass enhancement factors, explaining the differences as due to the anisotropic EPC (reported measurements in different directions) or to surface contamination. What is obviously needed is a re-evaluation of theoretical procedures for the calculation of EPC.

There are at least three possible explanations for the inconsistency in the published values of λ : (1) λ is anisotropic in k space (the reported λ 's were measured at inequivalent points on the Fermi contour), (2) the deviations in reported λ 's are caused by the different methods used to extract it

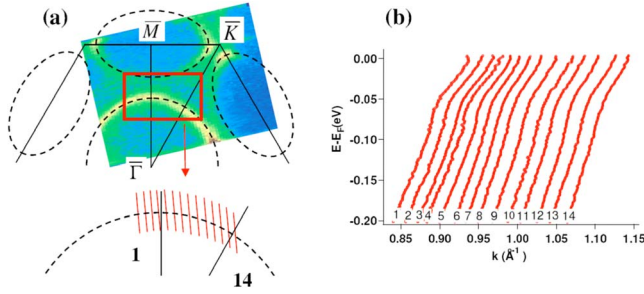


FIG. 1. (Color online) (a) Upper: photoemission intensity at the Fermi surface in the corresponding half of the hcp surface Brillouin zone of Be(0001). The dashed lines show the expected Fermi contours of the surface states. Lower: the zoom-in view of the $\bar{\Gamma}$ state Fermi contour with red lines indicating the cuts used for the high-resolution measurements and the determination of the EPC. (b) Surface-state dispersion along these cuts as determined from the maxima in the momentum distribution curves.

from the data, and (3) the quality of the data may affect the extracted value of λ . In the following we show that the EPC associated with the $\bar{\Gamma}$ surface state on Be(0001) is, in fact, anisotropic. We also illustrate how the resulting value of λ can be influenced by the method used to extract it and we finally argue that oxygen contamination is a likely reason for one of the observed low λ values.

ARPES experiments were performed at the SGM-3 beamline of the synchrotron radiation source ASTRID in Aarhus, Denmark.¹⁵ The total-energy resolution was set to ~ 15 – 20 meV, the angular resolution of the analyzer was 0.2° , and the photon energy was 16 eV. The sample was cooled to approximately 70 K. The surface was cleaned by standard methods.¹³ In the final stages of cleaning oxygen contamination (the main contaminant) was monitored via the Be $1s$ core-level peak and the valence band. A very small amount of oxygen could always be detected in the valence band but it was confirmed not to influence the results presented here. At significantly higher levels of oxygen contamination, we have observed a diminished EPC strength in the valence band. The orientation of the sample was determined by low-energy electron diffraction and Fermi-surface mapping at 60 eV photon energy.

The upper part of Fig. 1(a) shows the photoemission intensity at the Fermi energy together with a sketch of the surface Brillouin zone and the expected Fermi contours (black dashed half circle and ellipses). There are two surface states crossing the Fermi energy. One is centered at $\bar{\Gamma}$ and gives rise to a circular Fermi contour with a radius of about 0.94 \AA^{-1} (the $\bar{\Gamma}$ state in the following). The other is centered at \bar{M} and gives rise to an elliptic Fermi contour. High-resolution data for the $\bar{\Gamma}$ state were taken at a photon energy of 16 eV for different points on the circular Fermi contour. The present experimental arrangement does not allow for the rotation of the sample around the surface normal such that it was not possible to measure radial cuts through every point on the Fermi surface. Instead, we have taken data along the 14 cuts shown in the lower part of Fig. 1(a). The cuts become more nonradial as the angle away from the $\bar{\Gamma}$ - \bar{M} direction

increases. In the following, we determine the dispersion and the EPC strength based on these cuts, ignoring their nonradial nature. Using simulated spectral functions for different possible scenarios of coupling strength and anisotropy, we have established that this leads only to very minor changes in the resulting λ , on the order of 0.01, which is negligible compared to the other uncertainties. We have also confirmed this by taking data for many nonradial cuts with $0.1^\circ/\text{step}$, covering the same region as shown in Fig. 1(a). This permits us to construct a three-dimensional data set through which radial cuts can be laid. The results from this method are very similar but they suffer from poor statistics because of the smaller time available per scan.

Dispersion curves along the different cuts were determined by fitting the peak positions of the momentum distribution curves (MDCs) with Lorentz function. The result is shown in Fig. 1(b). Each curve displays a “kinklike” behavior, which is the signature of EPC renormalization of the bare particle dispersion.^{6,8–12,14,16–22} A qualitative examination of Fig. 1(b) indicates that the kink positions in all the dispersion curves occur at about the same energy, ~ 60 meV, agreeing with the results in the literature.^{8–12}

For a more detailed analysis, the complex self-energy Σ associated with the EPC has to be extracted from the experimental data. The real part of the self-energy, $\text{Re } \Sigma$, is given by the renormalization of the band, i.e., by the deviation of the actual dispersion from the so-called bare particle dispersion, which would be observed in the absence of EPC.²² We assume that the bare dispersion has a simple quadratic shape. The imaginary part of the self-energy, $\text{Im } \Sigma$, can be obtained from the Lorentz linewidth of the MDCs. Furthermore, $\text{Re } \Sigma$ and $\text{Im } \Sigma$ are related by a Kramers-Kronig transformation. We use this relation here in order to find the bare dispersion: the bare dispersion is obtained from a fit to the data at high binding energies and at the Fermi level (i.e., in regions where $\text{Re } \Sigma$ is small), with the boundary condition that the resulting $\text{Re } \Sigma$ must be consistent with $\text{Im } \Sigma$.²³ The final $\text{Re } \Sigma$ for the 14 cuts are shown in Fig. 2. Substantial differences are seen between these curves; some are broader than the others (such as cut 7 compared to cut 5) and different fine structure appears to be present despite the high noise level. This already indicates that the details of the EPC are not isotropic around the circular Fermi contour.

The next step of the analysis is to extract the mass enhancement factor from the self-energy. As a consistency check, and in order to evaluate the influence of the chosen approach on the result, we try three different methods.

(1) The most straightforward procedure is to determine λ from the slope of $\text{Re } \Sigma$ at the Fermi energy. This slope method is based on the basic relationship between the mass enhancement factor and $\text{Re } \Sigma$: $\lambda = \partial \text{Re } \Sigma(\omega, T) / \partial \omega|_{\omega=E_F; T=0}$. However, since this method strictly requires taking the derivative at zero energy and zero temperature, great care needs to be used when applying it. First, the measured dispersion near Fermi energy can be distorted due to the finite energy resolution and this may affect the resulting $\text{Re } \Sigma$ and λ .²² Second, the finite temperature will reduce the slope of $\text{Re } \Sigma$ near Fermi energy,¹⁴ leading to a systematic underestimate of λ . In the present case of Be(0001), neither restriction poses a severe problem because of the relatively high resolution and

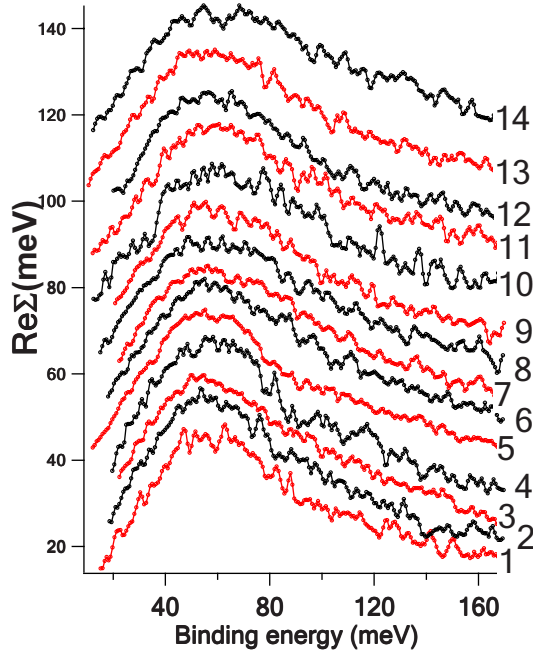


FIG. 2. (Color online) Extracted $\text{Re } \Sigma$, obtained from the dispersion relation shown in Fig. 1(b) by subtracting the bare dispersion. The kink positions are around 60 meV for all $\text{Re } \Sigma$. The curves have been displaced vertically for a clearer presentation.

low temperature, compared to the Debye temperature of ~ 1000 K. Hence, the slope method provides a simple and valuable test here.

(2) The most fundamental function for the description of the EPC is the Eliashberg coupling function $\alpha^2 F(\omega)$, which is related to the phonon density of states and the coupling strength.^{21,22,24} All other quantities of interest, including Σ and λ , can be derived from $\alpha^2 F(\omega)$. A common approach to determine λ is to assume a simple model for $\alpha^2 F(\omega)$, calculate $\text{Re } \Sigma$, and compare it to the experimental result. In such a procedure λ has the role of a fitting parameter. More precisely, one calculates

$$\text{Re } \Sigma(\omega; T) = - \int_{-\infty}^{\infty} d\nu \int_0^{\omega_{\max}} d\omega' \alpha^2 F(\omega') (2\omega' / \nu^2 - \omega'^2) \times f(\nu + \omega), \quad (1)$$

where $f(\omega)$ is the Fermi-Dirac distribution function. For $\alpha^2 F(\omega)$ one commonly uses a two- or three-dimensional Einstein or Debye model. Here, we use a two-dimensional Debye model, for which $\alpha^2 F(\omega) = \lambda(\omega/2\omega_D)$, where ω_D is the Debye frequency of the phonon mode that couples to the electrons. The shortcomings of this approach are the fact that the model for $\alpha^2 F(\omega)$ is largely arbitrary and, closely related, that essential model parameters such as the Debye or Einstein temperatures are unknown. In the following, this method of obtaining λ is referred to as the Debye method.

(3) The Eliashberg function can also be extracted directly from the measured $\text{Re } \Sigma$ by an integral inversion using the maximum entropy method (MEM).²¹ Once the Eliashberg function is extracted, the mass enhancement factor can be deduced from^{21,22,24}

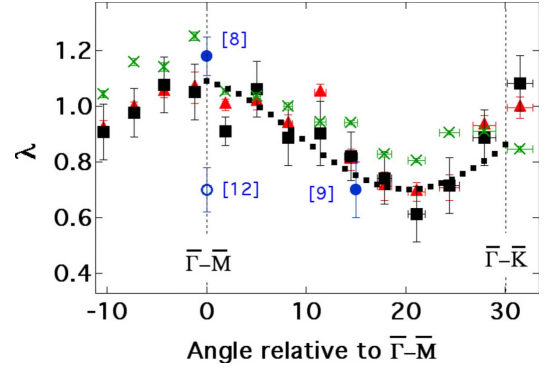


FIG. 3. (Color online) Mass enhancement factors as extracted from $\text{Re } \Sigma$ in Fig. 2 by MEM (solid squares), slope method (solid triangles), and Debye model method (crosses). The dashed line is a guide to the eye for the MEM results. The circles are values of λ reported in the literature; in the $\bar{\Gamma}-\bar{M}$ direction, the solid circle is determined from the slope of $\text{Re } \Sigma$ at E_F (Ref. 8), and the open circle by MEM (Ref. 12); the point in between $\bar{\Gamma}-\bar{M}$ and $\bar{\Gamma}-\bar{K}$ was extracted by fitting $\text{Re } \Sigma$ to a three-dimensional Debye model (Ref. 9).

$$\lambda = 2 \int_0^{\omega_{\max}} (\alpha^2 F(\omega') / \omega') d\omega', \quad (2)$$

where ω_{\max} is the top of the phonon bands.

Figure 3 shows the resulting mass enhancement factors extracted from the data presented in Fig. 2 using the MEM (solid squares), slope method (solid triangles), and Debye method (crosses). The dashed line is a guide to the eye for the MEM results. The results of all three models show that the mass enhancement is anisotropic in k space and even the absolute differences between the methods are mostly small. The mass enhancement factor has a global maximum in the $\bar{\Gamma}-\bar{M}$ direction (~ 1.1 from MEM) and a local maximum in the $\bar{\Gamma}-\bar{K}$ direction (~ 0.9 from MEM). The minimum lambda value appears $\sim 10^\circ$ away from the $\bar{\Gamma}-\bar{K}$ direction (~ 0.6 from MEM). The values extracted using the Debye model are, on average, ~ 0.1 larger than the values obtained from MEM. The values from the slope method are similar to the values from MEM.

The most important result of Fig. 3 is that the EPC is indeed anisotropic. While a different choice of extraction method can have an influence on the resulting λ in a given direction, the application of any method on the entire data set gives qualitatively the same anisotropy. Note, however, that the aforementioned restrictions for the slope method and the approach using a Debye model still apply and we believe the MEM result to be the most reliable, also in general.

A fundamental drawback when using a simple Debye or Einstein model for $\alpha^2 F(\omega)$ is that it cannot capture the complexity of $\alpha^2 F(\omega)$, leading to uncertainties in the determination of λ . This is illustrated in Fig. 4 which shows the experimental $\text{Re } \Sigma$ and models for the 14th cut, where a noticeable difference exists between λ deduced from the slope method, the MEM approach, and the Debye model (see Fig. 3). The experimental $\text{Re } \Sigma$ contains at least two major

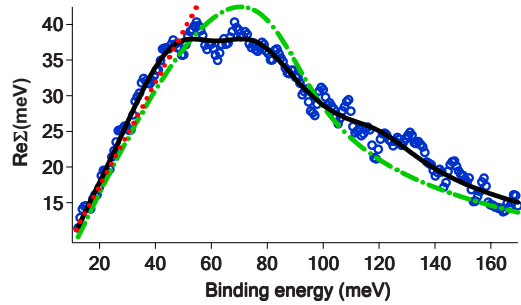


FIG. 4. (Color online) $\text{Re}\Sigma$ of cut 14 (blue circles) and Debye model fit (green dashed-dotted line), MEM fit (black solid line), and slope near the Fermi energy (red dotted line).

peaks: one in the 40–50 meV range and the other at ~ 70 meV, but $\text{Re}\Sigma$ in a Debye model has only a single maximum. An optimized fit of the whole curve with a single Debye frequency requires a Debye frequency higher than the dominant low-energy mode in the data. The unavoidable consequence is a reduction in the slope of the fitted $\text{Re}\Sigma$ at the Fermi energy and thus of the λ value evaluated from this method.

The MEM procedure, on the other hand, is constructed such that it can fit the whole $\text{Re}\Sigma$ curve, as seen in Fig. 4. In particular, it always results in a good fit for the important low-energy region, even in case of complicated structure in $\alpha^2F(\omega)$ at higher energies. In the present case, one might get the impression that the MEM approach is just a more sophisticated version of the slope method, but this is incorrect: the MEM approach to determining λ is not restricted to low temperatures (compared to the Debye temperature) because it determines the (temperature-independent) Eliashberg function rather than the (temperature-dependent) self-energy. Indeed, λ is extracted using Eq. (2), which is independent of the temperature. Ideally, one would like to determine fine structure in the Eliashberg function in order to infer which particular phonon modes are involved in the EPC on a specific point of the Fermi contour. Unfortunately, the signal to

noise ratio in our experiment is too low for a reliable determination of such a fine structure. The mass enhancement, on the other hand, is very robust against the noise.

Finally, we compare our results with the published EPC strength for different points on the Fermi surface. The previously reported values of λ are included in Fig. 3 as circles. Overall, earlier experimental findings agree reasonably well with our results. A notable exception is the data point from Ref. 12 which reports a smaller value of λ . Our own tests done in the present study as well as a reanalysis of the data of Ref. 12 suggest that this small value of λ is caused by oxygen contamination. The data point from Ref. 8 reporting a value of $\lambda = 1.18$ in the $\bar{\Gamma}-\bar{M}$ direction agrees very well with our results. The same group remarked in a later paper¹¹ that no significant differences could be observed between the $\bar{\Gamma}-\bar{M}$ and the $\bar{\Gamma}-\bar{K}$ directions, indicating that λ should be similar in both directions, consistent with our findings.

In conclusion, our work shows that electron-boson coupling can be anisotropic even in a simple two-dimensional system with a circular Fermi surface. The anisotropy could originate from the anisotropic nature of phonon dispersion and/or other electronic states (\bar{M} state or bulk states), which serve as final state of the EPC. The explanation must come from the details of the matrix element coupling^{24,25} in \mathbf{k} and \mathbf{q} .²⁵ So far there is no theoretical guidance of the nature of this coupling at the surface of Be. These data are an ideal test for various theoretical schemes.² The next step would be a comparison of the momentum-dependent Eliashberg functions. Experimentally, data with considerably better statistics would permit the extraction of the momentum-dependent Eliashberg function.

The work at Aarhus, Denmark was supported by the Danish National Research Council and the Lundbeck Foundation. T.Y.C. appreciates the financial support from his Tennessee Advanced Materials Laboratory (TAML) Grant. T.Y.C. and E.W.P. were supported by a joint grant from NSF and DMS&E of DOE (Grant No. NSF-DMR-04511632).

- ¹Y. Tokura and N. Nagaosa, *Science* **288**, 462 (2000).
- ²M. Lazzeri *et al.*, *Phys. Rev. B* **78**, 081406 (2008).
- ³Ph. Hofmann *et al.*, *Surf. Sci.* **355**, L278 (1996).
- ⁴M. Lazzeri and S. de Gironcoli, *Surf. Sci.* **402-404**, 715 (1998).
- ⁵E. V. Chulkov (private communication); recent calculation indicates that the value published in Ref. 14 is a factor of 2 too large due to programming error.
- ⁶E. V. Chulkov *et al.*, *Surf. Sci.* **188**, 287 (1987).
- ⁷J. B. Hannon *et al.*, *Phys. Rev. B* **53**, 2090 (1996).
- ⁸M. Hengsberger *et al.*, *Phys. Rev. Lett.* **83**, 592 (1999).
- ⁹S. LaShell *et al.*, *Phys. Rev. B* **61**, 2371 (2000).
- ¹⁰T. Balasubramanian *et al.*, *Phys. Rev. B* **57**, R6866 (1998).
- ¹¹M. Hengsberger *et al.*, *Phys. Rev. B* **60**, 10796 (1999).
- ¹²S.-J. Tang *et al.*, *Phys. Status Solidi B* **241**, 2345 (2004).
- ¹³R. A. Bartynski *et al.*, *Phys. Rev. B* **32**, 1921 (1985).
- ¹⁴A. Eiguren *et al.*, *Phys. Rev. Lett.* **91**, 166803 (2003).
- ¹⁵S. V. Hoffmann *et al.*, *Nucl. Instrum. Methods Phys. Res. A* **523**, 441 (2004).
- ¹⁶T. Cuk *et al.*, *Phys. Status Solidi B* **242**, 11 (2005).
- ¹⁷N. Mannella *et al.*, *Nature (London)* **438**, 474 (2005).
- ¹⁸P. Zhang *et al.*, *Phys. Rev. Lett.* **94**, 225502 (2005).
- ¹⁹T. Valla *et al.*, *Phys. Rev. Lett.* **102**, 107007 (2009).
- ²⁰G. D. Mahan, *Many-Particle Physics*, 3rd ed. (Springer, Berlin, 2007).
- ²¹J. Shi *et al.*, *Phys. Rev. Lett.* **92**, 186401 (2004).
- ²²C. Kirkegaard *et al.*, *New J. Phys.* **7**, 99 (2005).
- ²³A. A. Kordyuk *et al.*, *Phys. Rev. B* **71**, 214513 (2005).
- ²⁴G. Grimvall, *The Electron-Phonon Interaction in Metals* (North-Holland, New York, 1981).
- ²⁵N. Bulut and D. J. Scalapino, *Phys. Rev. B* **54**, 14971 (1996).